Surface traction and the dynamics of elastic rods at low Reynolds number

Eva M. Strawbridge
Department of Mathematics, University of Chicago, Chicago, Illinois 60637, USA

Charles W. Wolgemuth
Department of Cell Biology and Center for Cell Analysis and Modeling, University of Connecticut Health Center, Farmington, Connecticut 06030-6406, USA

(Received 9 July 2012; published 5 September 2012)

Molecular and cell biological processes often use proteins and structures that are significantly longer in one dimension than they are in the other two, for example, DNA, actin, and bacterial flagella. The dynamics of these structures are the consequence of the balance between the elastic forces from the structure itself and viscous forces from the surrounding fluid. Typically, the motion of these filamentary objects is described using variations of the Kirchhoff rod equations with resistive forces from the fluid treated as body forces acting on the centerline. In reality, though, these forces are applied to the surface of the filament; however, the standard derivation of the Kirchhoff equations ignores surface traction stresses. Here, we rederive the Kirchhoff rod equations in the presence of resistive traction stresses and determine the conditions under which treating the drag forces as body forces is reasonable. We show that in most biologically relevant cases the standard implementation of resistive forces into the Kirchhoff rod equations is applicable; however, we note one particular biological system where the Kirchhoff rod formalism may not apply.

DOI: 10.1103/PhysRevE.86.031904 PACS number(s): 87.85.gj, 47.63.−b, 47.15.G−

I. INTRODUCTION

The motion of thin, elastic objects at low Reynolds number has been an active area of research in the physics and applied mathematics communities for at least the last 30 years. These investigations have been primarily motivated by molecular and cellular biology, where many important structures, such as DNA, actin, microtubules, and bacterial flagella, are much longer in one dimension than they are in the other two. The ability to mathematically model the dynamics of these biological structures is necessary for determining the shape, dynamics, or material parameters of biomolecules or materials [1–29], investigating mechanisms involved with the swimming of flagellated (usually micro-) organisms [11,21,22,30–33], or studying the growth of biofilaments [14,34,35]. Since all of these biofilaments are immersed in fluids, fluid-structure interactions govern their dynamics.

To fully solve for the motion of an elastic filament immersed in a fluid, though, requires an accurate treatment of both the solid mechanics of the filament and the hydrodynamics of the fluid. Asymptotic theories have been developed separately to describe either the elasticity of long, thin objects or the fluid flows about these filaments. For example, the Kirchhoff rod equations [36–42] (also called the Kirchhoff-Clebsch equations) are an asymptotic theory designed to elucidate the dynamics of a slender three-dimensional object which allows large-scale twist and bend. These equations exploit the slenderness by assuming limitations on the global and local internal deformations, which then allows the dynamics of the three-dimensional body to be described purely through the bend of and rotation about the one-dimensional centerline, a reduction in dimension that has clear advantages in analysis and implementation. In a similar fashion, slender-body hydrodynamics exploit the slenderness of a filament to asymptotically determine the fluid flows about a thin, three-dimensional object either through the local velocity of the filament with resistive force theory [44,45] or with both local and nonlocal contributions through slender-body theory [46–48]. In both resistive force and slender-body theory, the fluid flows can then be used to show that the leading order force per length on a filament is proportional to the local velocity of the filament centerline [49].

A traditional method for handling the coupled solid and fluid mechanics that accompany motions of filamentary objects through fluids is to balance the elastic restoring forces derived from the Kirchhoff equations with the resistive forces derived from the leading order term in slender-body theory (see, for example, [14,32,49]). This methodology, however, effectively treats the resistive forces from the fluid as a body force that is exerted on the filament. In reality, the fluid forces arise from traction forces exerted on the surface of the filament. A concern then arises since the derivation of the Kirchhoff equations relies on assuming zero surface traction as a boundary condition. What then is the correct formalism for coupling fluid resistance into the Kirchhoff rod equations?

Here we investigate this question. We show that the traditional approach (where surface traction is treated as a body force) does, in fact, result in the same dynamics as when the fluid forces are treated precisely as surface tractions. The significance of our approach, however, is that it naturally provides explicit bounds on the filament velocity, above which the assumptions of Kirchhoff rod theory are no longer applicable. We show that the constraint on the velocity depends predominantly on the shear modulus of the filament, and that in most biologically relevant scenarios the Kirchhoff rod equations can be used to describe the motions of biofilaments. However, in the Conclusion, we note one particular biological system that has received recent interest which may exceed the velocity constraint derived here.

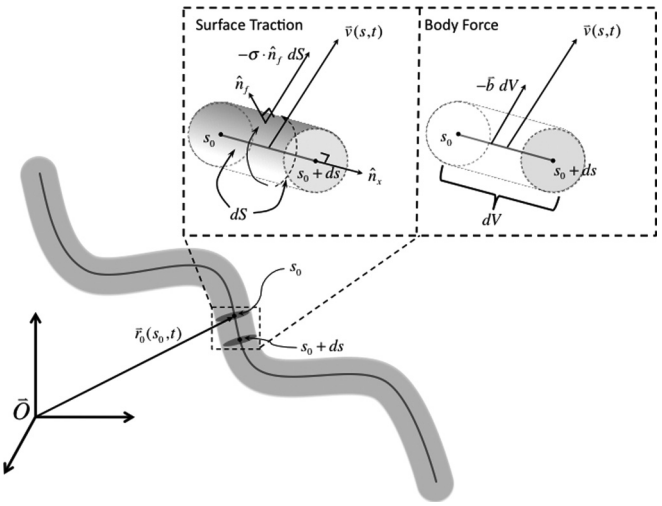

FIG. 1. The centerline of the slender body given by the vector $\mathbf{r}_0(s,t)$ from a fixed origin $\vec{\mathbf{O}}$. The velocity of the centerline is given by $\mathbf{v}(s,t) = \frac{\partial \mathbf{r}_0}{\partial t}(s,t)$. Inset: an infinitesimal segment of the rod of length ds where the traction schemes may be treated as either surface or body forces, respectively. When treated as a surface traction (left panel) the force is applied everywhere on the infinitesimal surface dS of the rod segment between arclength points s_0 and $s_0 + ds$. When treated as a body force the force is effectively felt at the centerline after integrating over the finite volume element dV.

II. THE KIRCHHOFF ROD EQUATIONS WITH SURFACE TRACTION

In order to analyze the effect of fluid resistance in the Kirchhoff rod model we begin by scrutinizing the physical and mathematical differences between treating the resistive drag force as a body force versus treating it accurately as a surface traction stress. We consider a thin filament of length L with centerline position defined by the vector $\mathbf{r}_0(s,t)$, where s is the arclength and t is time (Fig. 1). Material points in the filament are then given by $\mathbf{r}(s,t) = \mathbf{r}_0(s,t) + x_\alpha \hat{\mathbf{e}}_\alpha(s,t) + u_k(x_1,x_2,s,t)\hat{\mathbf{e}}_k(s,t)$, where $0 \leqslant s \leqslant L$ is the arclength and $\hat{\mathbf{e}}_1$ and $\hat{\mathbf{e}}_2$ are orthogonal unit vectors that lie in the plane perpendicular to the tangent vector to the centerline, $\hat{\mathbf{e}}_3$. For this paper we use the convention that repeated indices α and β are summed from 1 to 2 and all other indices are summed from 1 to 3. The quantities $x_1 + u_1(x_1,x_2,s,t)$ and $x_2 + u_2(x_1,x_2,s,t)$ define the perpendicular distance from the centerline to the material point while $u_3(x_1,x_2,s,t)$ is the deformation of the cross-section from planar. For an inextensible rod, we require $\mathbf{u}(0,0,s,t) = u_k(0,0,s,t)\hat{\mathbf{e}}_k(s,t) = \mathbf{0}$.

We define the characteristic size of the cross-section to be a, such that the maximum magnitudes of x_1 and x_2 are approximately equal to a. If the rod is circular, $0 \leqslant x_\alpha \leqslant a$. For this characteristic size, we consider $\epsilon \equiv \max\{a/L, a/C, a|\boldsymbol{\kappa}|\}$ and $\epsilon \ll 1$, where $\boldsymbol{\kappa}$ is the rate of bend and twist along the rod ($\frac{\partial \hat{\mathbf{e}}_k}{\partial s} = \boldsymbol{\kappa} \times \hat{\mathbf{e}}_k$) and C is the radius of curvature.

If the rod is immersed in a fluid at low Reynolds number, the inertial terms in the balance of momentum equations for both the fluid and the rod are expected to be negligible. Therefore, the balance of linear momentum of the rod requires that the divergence of the elastic stress, $\nabla \cdot \boldsymbol{\sigma}_e$, of the rod must be balanced by any body forces acting on the rod, $\mathbf{b}$:

$$\nabla \cdot \boldsymbol{\sigma}_e + \mathbf{b} = 0. \tag{1}$$

The boundary conditions for Eq. (1) are that the elastic stresses at the surface of the rod are equal to the traction stresses applied to its external surface:

$$\boldsymbol{\sigma}_e \cdot \hat{\mathbf{n}} = \boldsymbol{\tau}, \tag{2}$$

where $\hat{\mathbf{n}}$ is the outward normal to the surface, and $\boldsymbol{\tau}$ is the traction stress. Figure 1 depicts an illustration of these two approaches.

A. The traditional implementation of resistive forces in the Kirchhoff equations

In the traditional derivation of the Kirchhoff rod equations, $\boldsymbol{\tau}$ is assumed to be zero. To derive the approximate equations that govern the motion of the centerline, Eq. (1) is integrated over the volume dV of an infinitesimal length of the rod, ds, i.e.,

$$\begin{aligned}
&\int (\nabla \cdot \boldsymbol{\sigma}_e + \mathbf{b})\, dV = 0,\\
&\int \left(\boldsymbol{\sigma}_e \cdot \hat{\mathbf{n}}_\mathrm{f}\right) dA_\mathrm{f} + \int (\boldsymbol{\sigma}_e \cdot \hat{\mathbf{n}}_\mathrm{x})\, dA_\mathrm{x}|_s\\
&\quad + \int (\boldsymbol{\sigma}_e \cdot \hat{\mathbf{n}}_\mathrm{x})\, dA_\mathrm{x}|_{s+ds} = -\int \mathbf{b} dV,\\
&\int (\boldsymbol{\sigma}_e \cdot \hat{\mathbf{n}}_\mathrm{x})\, dA_\mathrm{x}|_s + \int (\boldsymbol{\sigma}_e \cdot \hat{\mathbf{n}}_\mathrm{x})\, dA_\mathrm{x}|_{s+ds} = -\int \mathbf{b} dV,
\end{aligned} \tag{3}$$

where the subscripts "f" and "x" denote the exterior surface of the rod (i.e., the surface that is in contact with the fluid) and the surface defined by the cross-sections of the infinitesimal length of the rod, respectively. The normals to the surfaces are $\hat{\mathbf{n}}_\mathrm{f}$ and $\hat{\mathbf{n}}_\mathrm{x}$. The integrals over the cross-sectional areas are evaluated at s and $s + ds$, and the last line of Eq. (3) is a consequence of assuming that the traction stress is zero, which requires any surface traction forces, such as resistive forces from the fluid, to be treated as body forces.

It is standard to assume that the cross-sections remain approximately circular and planar. That is, $\frac{u_k}{a} = O(\epsilon) = \frac{\partial u_k}{\partial x_\alpha}$ and $\frac{\partial u_k}{\partial s} = O(\epsilon^2)$ (these are essential to enforce local injectivity of the body representation $\mathbf{r}$). As a result of this and an appropriate constitutive relation, the stresses are at most order ϵ [42]. In this case, the normal vectors for the cross-sections are approximately parallel to the tangent vector of the centerline of the filament. It is, therefore, possible to rewrite Eq. (3) as

$$ds \frac{\partial}{\partial s}\left(\int (\boldsymbol{\sigma}_e \cdot \hat{\mathbf{e}}_3)\, dA_\mathrm{x}\right) = -\int \mathbf{b} dV, \tag{4}$$

by dropping all terms of order ϵ^2 or higher. The integral on the left-hand side of Eq. (4) is the elastic restoring force that acts on the cross-section, $\mathbf{F} = \int (\boldsymbol{\sigma}_e \cdot \hat{\mathbf{e}}_3) dA_\mathrm{x}$, which can be considered to be localized at the center of the cross-section. From this definition for the force, it is straightforward to show that the force is related to the moment as $\mathbf{F} \times \hat{\mathbf{e}}_3 = \partial \mathbf{M}/\partial s$, where the moment is $\mathbf{M} = \int [x_\alpha \hat{\mathbf{e}}_\alpha \times (\boldsymbol{\sigma}_e \cdot \hat{\mathbf{e}}_3)] dA_\mathrm{x}$ to order ϵ.

In this traditional formulation, the integral of the body force divided by ds is assumed to be equal to the force per length

that is derived from slender-body hydrodynamics, i.e.,

$$-\frac{1}{ds}\int \mathbf{b}dV = \zeta_\perp \mathbf{v} + \zeta_\parallel (\hat{\mathbf{e}}_3 \cdot \mathbf{v})\hat{\mathbf{e}}_3, \tag{5}$$

where $\mathbf{v}$ is the local velocity of the filament and $\zeta_\perp$ and $\zeta_\parallel$ are the drag coefficients for motion perpendicular to or parallel with the tangent vector, respectively. In other words, the integral of $\mathbf{b}$ is the total resistive force that acts on the infinitesimal length of the rod.

Combining Eqs. (4) and (5) with the balance of the moments and forces, we get the usual form of the low Reynolds number Kirchhoff rod equations with resistive drag:

$$\frac{\partial \mathbf{M}}{\partial s} + \hat{\mathbf{e}}_3 \times \mathbf{F} = \mathbf{0}, \tag{6}$$

$$\frac{\partial \mathbf{F}}{\partial s} = \zeta_\perp \mathbf{v} + \zeta_\parallel (\hat{\mathbf{e}}_3 \cdot \mathbf{v})\hat{\mathbf{e}}_3. \tag{7}$$

B. Resistive forces from surface traction

Resistive forces, however, arise from stresses that are exerted on the surface of the rod (the surface labeled "f"), not on volume elements inside the rod. Therefore, an accurate treatment of the effect of fluid drag forces should consider that the body forces on the filament are zero and that the normal component of the elastic stress at the surface of the rod is equal to traction stress from the fluid. Integrating Eq. (1) over an infinitesimal length of the filament then leads to

$$\begin{aligned}&\int \nabla \cdot \boldsymbol{\sigma}_e dV = 0,\\ &\int (\boldsymbol{\sigma}_e \cdot \hat{\mathbf{n}}_\mathrm{X})\, dA_\mathrm{X}|_s + \int (\boldsymbol{\sigma}_e \cdot \hat{\mathbf{n}}_\mathrm{X})\, dA_\mathrm{X}|_{s+ds}\\ &\quad = -\int (\boldsymbol{\sigma}_e \cdot \hat{\mathbf{n}}_\mathrm{f}) dA_\mathrm{f}.\end{aligned} \tag{8}$$

The integral on the right-hand side of Eq. (8) is equal to the total external force that is exerted on the surface of the infinitesimal length of the filament, i.e.,

$$-\frac{1}{ds}\int \boldsymbol{\tau} dV = \zeta_\perp \mathbf{v} + \zeta_\parallel (\hat{\mathbf{e}}_3 \cdot \mathbf{v})\hat{\mathbf{e}}_3, \tag{9}$$

where we have used the boundary condition given in Eq. (2). Therefore, including the resistive drag correctly as a surface traction should lead to the same force balance equation as is obtained when the resistive drag is treated as a body force. However, there remains a major difference, which is highlighted in the derivation of the relationship between the forces and moments and the deformation of the filament. While both approaches require additionally a constitutive relationship to relate the elastic stress in the filament to the filament displacements, the same constitutive relationship will lead to different deformations of the cross-sections due to the difference in the stress equations.

When resistive forces are treated as body forces, the stress satisfies $\nabla \cdot \boldsymbol{\sigma}_e = -\mathbf{b}$ with the boundary condition that $\boldsymbol{\sigma}_e \cdot \hat{\mathbf{n}} = 0$ on the surface of the rod. A scaling argument is also typically used to set the body forces normal to the centerline to zero on the surface of the rod (i.e., $\mathbf{b} \cdot \hat{\mathbf{e}}_3 \approx 0$), which places a further constraint on the size of the allowable body forces [42]. With this additional assumption and using a linear elastic constitutive relationship, a set of coupled differential equations (in x_1 and x_2 only) for the small deformations of the cross-section is obtained, which yields *exact* solutions for $\mathbf{u}$. A careful asymptotic treatment of the classical Kirchhoff equations was performed by Dill [42] and so will not be repeated here.

When the resistive forces arise from traction stresses, then $\nabla \cdot \boldsymbol{\sigma}_e = 0$ with boundary condition, $\boldsymbol{\sigma}_e \cdot \hat{\mathbf{n}} = \boldsymbol{\tau}$. To determine how the Kirchhoff rod equations are altered by surface traction, we need to compute the deformations of the filament using linear elasticity and the preceding stress equations.

In other words, while the force and moment balance equations remain the same, the relationship between the force and/or moment and the deformations of the filament can be different depending on how the resistive forces are handled. The implications of this when surface traction is present have not been fully addressed. In what follows, we use slender-body hydrodynamics to define the surface traction stress exerted on a thin filament moving through a viscous fluid at low Reynolds number as an expansion in ϵ. By describing the deformation of the filament using a similar expansion in ϵ and equating the normal components of the fluid and elastic stresses at the surface of the filament, we can solve for the deformations of the cross-section, which can then be used to relate the centerline shape of the filament to the elastic force per length. While our analysis assumes low Reynolds number, the same principles apply if the surrounding fluid has inertia.

III. DIMENSIONAL ANALYSIS

Before embarking on the full calculation of the effect of resistive forces on the constitutive relationship for the rod, we consider the physical implications of the surface traction boundary condition using scaling arguments. In linear elasticity theory, the stress is proportional to an elastic modulus, such as the Young's modulus, E, times time gradient of the displacement. Therefore, a characteristic size for the elastic stress is $\boldsymbol{\sigma}_e \sim Eu/a$, where u is a characteristic size of the deformations. Since the normal component of the elastic stress at the surface of the filament must equal the fluid stress, we can use Eq. (9) to relate the stress at the surface of the rod to the fluid stress: $Eu \sim \zeta_\perp v \sim \mu v$, where μ is the viscosity of the fluid. In order to preserve the assumptions that underlie the derivation of the force and moment balance equations, $u \sim a\epsilon < a^2/L$, the velocity of the filament is constrained such that $v < Ea^2/\mu L$. Many microorganisms swim by propagating traveling waves along the length of a filamentary object. The classic example is undulations of the flagellum of mammalian sperm [43]. For this case, the characteristic velocity of the filament is roughly equal to the undulation frequency, ω, times the length of the flagellum, L. Therefore, our dimensional analysis constraint on the velocity can be recast as a constraint on a dimensionless number, $\eta\omega L^2/Ea^2 < 1$. This dimensionless number is equivalent to the "sperm number," $\mathrm{Sp} = L(\omega\zeta_\perp/A)^{\frac{1}{4}}$, to the fourth power divided by the square of the aspect ratio, ϵ^2, where the bending modulus is proportional to the Young's modulus as $A \sim a^4 E$ [43]. Therefore, $\mathrm{Sp}^4/\epsilon^2 < 1$. As we will show below, this estimate for the velocity at which the Kirchhoff rod assumptions break down is fairly accurate; however, the

full analysis reveals that the condition is determined by the shear modulus, S, not the Young's modulus.

IV. SURFACE TRACTION AND THE CONSTITUTIVE RELATIONSHIP OF ELASTIC RODS

A. The constitutive relation

As alluded to already, the difference between treating resistive forces from the environment as a surface traction, instead of as a body force, lies in the determination of the small strains, $\mathbf{u}$. The solution to these strains in conjunction with the stress equations then leads to a formulation for the moment $\mathbf{M}$ and force $\mathbf{F}$ that relates forces and torques on the centerline of the filament to the curvature and twist. In our preceding derivation of the force and moment from the stress, we made no assumptions regarding the relationship between the stress and strain. In most cases in the literature, the filament is assumed to obey linear elasticity, and, therefore,

$$\sigma_{km} = 2S\mathcal{E}_{km} + \lambda\mathcal{E}_{ii}\delta_k^m, \tag{10}$$

where the strain tensor $\mathcal{E}_{km}$ can be readily approximated to order ϵ from the deformation gradient of the body, $(\nabla\mathbf{u} + (\nabla\mathbf{u})^T)/2$, where the superscript T denotes the transpose. Here $\lambda = 2S\nu/(1-2\nu)$ relates the shear modulus and Poisson's ratio, $\nu = E/2S - 1$. The components of the stress tensor to order ϵ are then

$$\sigma_{11} = (2S+\lambda)\frac{\partial u_1}{\partial x_1} + \lambda\left[\frac{\partial u_2}{\partial x_2} + \left(-\kappa_2+\kappa_2^0\right)x_1 + \left(\kappa_1-\kappa_1^0\right)x_2\right], \tag{11a}$$

$$\sigma_{12} = S\left(\frac{\partial u_1}{\partial x_2} + \frac{\partial u_2}{\partial x_1}\right), \tag{11b}$$

$$\sigma_{13} = S\left[\frac{\partial u_3}{\partial x_1} + \left(-\kappa_3+\kappa_3^0\right)x_2\right], \tag{11c}$$

$$\sigma_{22} = (2S+\lambda)\frac{\partial u_2}{\partial x_2} + \lambda\left[\frac{\partial u_1}{\partial x_1} + \left(-\kappa_2+\kappa_2^0\right)x_1 + \left(\kappa_1-\kappa_1^0\right)x_2\right], \tag{11d}$$

$$\sigma_{23} = S\left[\frac{\partial u_3}{\partial x_2} + \left(\kappa_3-\kappa_3^0\right)x_1\right], \tag{11e}$$

$$\sigma_{33} = (2S+\lambda)\left[\left(-\kappa_2+\kappa_2^0\right)x_1 + \left(\kappa_1-\kappa_1^0\right)x_2\right] + \lambda\left(\frac{\partial u_1}{\partial x_1} + \frac{\partial u_2}{\partial x_2}\right), \tag{11f}$$

where $\boldsymbol{\kappa}^0$ is the curvature and twist of the reference configuration.

B. Classical Kirchhoff theory

Classical Kirchhoff theory is usually simply stated as the relationships for the elastic force and moment experienced at the filament centerline [e.g., Eq. (7)] plus the relationship between the resultant torque and the local bend and twist, i.e.,

$$\mathbf{M} = \frac{EJ}{2}\left(\kappa_\alpha - \kappa_\alpha^0\right)\hat{\mathbf{e}}_\alpha + SJ\left(\kappa_3-\kappa_3^0\right)\hat{\mathbf{e}}_3, \tag{12}$$

where J is the massless moment of inertia for a rod with circular cross-section. Equation (12) is often referred to as being equivalent to linear elasticity. However, this is not precisely true, as Eq. (12) requires linear elasticity [i.e., Eq. (10)] along with the assumptions regarding the smallness of ϵ and the deformations $\mathbf{u}$, as well as a negligible normal component of the stress on the surface of the cross-section. That is, Eq. (12) requires both Eq. (10) as well as the following:

$$\frac{\partial\sigma_{\alpha k}}{\partial x_\alpha} = O(\epsilon^2) \text{ with } n_\alpha\sigma_{\alpha k} = 0. \tag{13}$$

While arguments can and have been made to justify these additional assertions, all such reasoning makes implicit assumptions as to the allowable size of external surface and body forces. For the case of resistive forces from the environment, these assumptions indirectly limit the magnitude of the velocity of the filament (as estimated in Sec. III). However, if these assumptions are justified, then Eq. (13) can be used to solve for the small deformations, $\mathbf{u}$, through a set of homogeneous partial differential equations (in the cross-sectional variables only) with zero boundary conditions. These equations can be solved exactly and yield

$$u_1 = -\nu\left(\kappa_1-\kappa_1^0\right)x_1x_2 + \frac{\nu}{2}\left(\kappa_2-\kappa_2^0\right)\left(x_1^2-x_2^2\right), \tag{14a}$$

$$u_2 = \nu\left(\kappa_2-\kappa_2^0\right)x_1x_2 + \frac{\nu}{2}\left(\kappa_1-\kappa_1^0\right)\left(x_1^2-x_2^2\right), \tag{14b}$$

$$u_3 = 0, \tag{14c}$$

for a circular cross-section. Employing these solutions for $\mathbf{u}$ yields the resultant torque, Eq. (12). However, it is not necessarily obvious that Eq. (12) holds if the conditions in Eq. (13) are not satisfied.

C. Deformations from resistive surface tractions

In order to solve for the deformations, $\mathbf{u}$, when surface traction is present, we look for solutions as an expansion in the transverse coordinates x_1 and x_2:

$$u_k \approx u_k^{(0)} + u_k^{(1)}x_1 + u_k^{(2)}x_2 + u_k^{(3)}x_1x_2 + \frac{u_k^{(4)}}{2}x_1^2 + \frac{u_k^{(5)}}{2}x_2^2 + u_k^{(6)}x_1^2x_2 + u_k^{(7)}x_1x_2^2 + \frac{u_k^{(8)}}{3}x_1^3 + \frac{u_k^{(9)}}{3}x_2^3. \tag{15}$$

In this expansion, we set the spatially independent terms $u_k^{(0)} = 0$ for $k \in \{1,2,3\}$, since nonzero values represent a rigid translation of the centerline and, therefore, do not describe strains in the filament.

1. The local fluid velocity

In order to solve for the displacements, we need to specify the surface tractions. Our interest is in determining the proper Kirchhoff rod equations for thin filaments moving through viscous fluids. We, therefore, consider a filament moving through a low Reynolds number fluid that is governed by the Stokes equations. We can then use the resistive-force theory (i.e., using only the zeroth order terms with local velocities) of Keller and Rubinow [47] to describe the near-field fluid

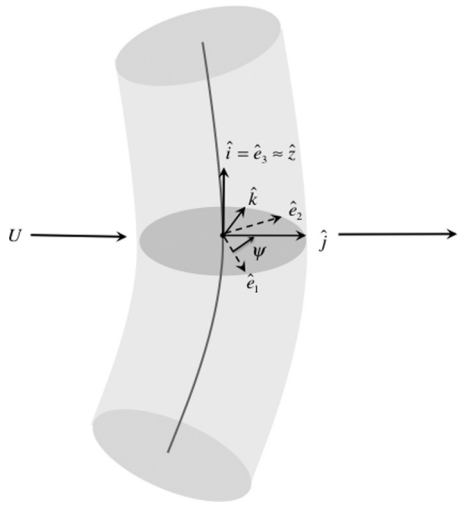

FIG. 2. A short segment of the rod depicting the Kirchhoff frame $\{\hat{\mathbf{e}}_i\}$, the Keller-Rubinow frame $\{\hat{\mathbf{i}},\hat{\mathbf{j}},\hat{\mathbf{k}}\}$, and the counterclockwise rotation ψ of $\hat{\mathbf{e}}_1$ to the unit vector $\hat{\mathbf{j}}$ in the direction of the fluid flow with velocity $\mathbb{U}$.

velocity, which is given to lowest order by

$$\begin{aligned}\mathbb{U}(\mathbf{x}) \approx{}& \mathbb{U}_0(s) + \hat{\mathbf{i}}(s)\beta(s)\log\left(\frac{\rho}{a}\right)\\ &+\hat{\mathbf{j}}(s)\gamma(s)\left[\log\left(\frac{\rho}{a}\right)+\frac{1}{2}\left(1-\frac{a^2}{\rho^2}\right)\right]\\ &-[\hat{\mathbf{j}}(s)\cos^2\theta+\hat{\mathbf{k}}(s)\sin\theta\cos\theta]\gamma(s)\left(1-\frac{a^2}{\rho^2}\right)\\ &+[-\hat{\mathbf{j}}(s)\sin\theta+\hat{\mathbf{k}}(s)\cos\theta]\frac{\xi(s)a^2}{\rho},\end{aligned} \tag{16}$$

where $\hat{\mathbf{i}} = \hat{\mathbf{e}}_3$, $\hat{\mathbf{j}}$ is in the direction of the fluid flow normal to the the centerline and ρ and θ are the local polar coordinates internal in the plane of the cross-section of the rod. The relationship between the coordinate frames is depicted schematically in Fig. 2 (this is the local coordinate system used by Keller and Rubinow [47]). The first term in Eq. (16) is the translational velocity at the surface of the rod, and the second term is the translational velocity parallel to the centerline. The third and fourth terms are the translational velocity normal to the centerline, and the fifth term is the velocity due to rotation. The angle ψ is the counterclockwise rotation of $\hat{\mathbf{e}}_1$ to $\hat{\mathbf{j}}$. Hence,

$$\begin{aligned}\hat{\mathbf{z}} &= \hat{\mathbf{e}}_3,\\ \hat{\rho} &= \cos(\theta+\psi)\hat{\mathbf{e}}_2 + \sin(\theta+\psi)\hat{\mathbf{e}}_2,\\ \hat{\theta} &= -\sin(\theta+\psi)\hat{\mathbf{e}}_1 + \cos(\theta+\psi)\hat{\mathbf{e}}_2.\end{aligned}$$

The parameters β, γ, ξ, and the third director $\hat{\mathbf{k}} = \hat{\mathbf{i}}\times\hat{\mathbf{j}}$ are approximated to lowest order by matching the asymptotic expansions between the near- and far-field fluid velocities [47]. Only the fluid velocity normal to the centerline produces a nonconstant pressure $P = \frac{2\mu\gamma}{a}\cos\theta$.

2. The stress at the surface of the rod

The surface traction that the fluid exerts on a translating and rotating filament can be computed using the velocity field given in Eq. (16) and the viscous fluid stress tensor:

$$\boldsymbol{\sigma}_f = \mu(\nabla\mathbb{U} + (\nabla\mathbb{U})^T) + P\boldsymbol{\mathcal{I}}, \tag{17}$$

where P is the fluid pressure and $\boldsymbol{\mathcal{I}}$ is the identity matrix. The surface traction is then obtained from the normal component of the stress evaluated at the surface of the filament:

$$\boldsymbol{\tau}_{\hat{\mathbf{n}}} = -P\hat{\mathbf{n}} + \mu[2(\hat{\mathbf{n}}\cdot\nabla)\mathbb{U} + \hat{\mathbf{n}}\times(\nabla\times\mathbb{U})].$$

Setting the surface normal to be $\hat{\mathbf{n}} = \hat{\rho}$ at $\rho = a$ and rotating into the $\hat{\mathbf{e}}_k$ basis yields

$$\begin{aligned}\boldsymbol{\tau}_{\text{fluid}} ={}& [K_1\cos\psi + K_2\sin(\theta+\psi)]\,\hat{\mathbf{e}}_1\\ &+[K_1\sin\psi - K_2\cos(\theta+\psi)]\,\hat{\mathbf{e}}_2 + K_3\hat{\mathbf{e}}_3,\end{aligned} \tag{18}$$

where $K_1 = \frac{2\mu\gamma}{a}$, $K_2 = 2\mu\xi$, and $K_3 = \frac{\mu\beta}{a}$. The stress on the surface of the rod is then

$$\begin{aligned}\boldsymbol{\tau}_{\text{rod}} ={}& [\sigma_{11}\cos(\theta+\psi) + \sigma_{12}\sin(\theta+\psi)]\,\hat{\mathbf{e}}_1\\ &+[\sigma_{12}\cos(\theta+\psi) + \sigma_{22}\sin(\theta+\psi)]\,\hat{\mathbf{e}}_2\\ &+[\sigma_{13}\cos(\theta+\psi) + \sigma_{23}\sin(\theta+\psi)]\,\hat{\mathbf{e}}_3.\end{aligned} \tag{19}$$

Using Eqs. (11a)–(11f) and (15) in Eq. (19) and matching with the fluid stress, we compute the elastic deformations of the filament that are produced by the surface traction and the bending and twisting of the filament:

$$\begin{aligned}u_1 ={}& \left[-\nu\left(\kappa_1-\kappa_1^0\right) - \frac{K_1}{2aS}\sin\psi\right]x_1x_2\\ &+\left[\nu\left(\kappa_2-\kappa_2^0\right)+\frac{K_1}{2aS}\cos\psi\right]\frac{x_1^2}{2}\\ &-\left[\nu\left(\kappa_2-\kappa_2^0\right)-\frac{3K_1}{2aS}\cos\psi\right]\frac{x_2^2}{2}\\ &+\frac{K_2}{2a^2S}x_2\left(x_1^2+x_2^2\right),\end{aligned} \tag{20a}$$

$$\begin{aligned}u_2 ={}& \left[\nu\left(\kappa_2-\kappa_2^0\right) - \frac{K_1}{2aS}\cos\psi\right]x_1x_2\\ &+\left[\nu\left(\kappa_1-\kappa_1^0\right)+\frac{3K_1}{2aS}\sin\psi\right]\frac{x_1^2}{2}\\ &-\left[\nu\left(\kappa_1-\kappa_1^0\right)-\frac{K_1}{2aS}\sin\psi\right]\frac{x_2^2}{2}\\ &-\frac{K_2}{2a^2S}x_1\left(x_1^2+x_2^2\right),\end{aligned} \tag{20b}$$

$$u_3 = \frac{K_3}{2aS}\left(x_1^2+x_2^2\right). \tag{20c}$$

It is worth noting here that if the drag is properly handled as a surface traction, then the cross-sections can only remain approximately planar (i.e., $u_3 \neq 0$).

D. Recovery of the classical theory

It is immediately clear that if the fluid viscosity is zero (i.e., the surface tractions are zero), then this method recovers the classical solutions for $\mathbf{u}$ given by Eqs. (14a)–(14c). Additionally, using the definitions of the resultant force $\mathbf{F}$ and torque $\mathbf{M}$ and the new solutions for the deformations, the classical relation [Eq. (12)] is also recovered. Furthermore, substituting these new solutions for the small deformations [Eqs. (20a)–(20c)] into the integral on

the right-hand side of Eq. (8) and dropping all but the largest terms reveals that $-2\pi a[K_1(\cos\psi\hat{\mathbf{e}}_1+\sin\psi\hat{\mathbf{e}}_2)+K_3\mathbf{e}_3]\approx\zeta_\perp\mathbf{v}+\zeta_\parallel(\hat{\mathbf{e}}_3\cdot\mathbf{v})\hat{\mathbf{e}}_3$, which is exactly Eq. (7) with $\mathbf{v}=\frac{\partial\mathbf{r}_0}{\partial t}$.

One clear benefit of this approach is that it makes explicit the size restrictions on the allowable velocities and validates our dimensional analysis. That is, in order for the derivation of the deformation gradient, the strain tensor, and subsequently the constitutive relations to hold, the small deformations must be $\frac{u_k}{a}=O(\epsilon)$. Hence,

$$\frac{\mu}{aS\log(L/a)}|v_\alpha|\lesssim\epsilon, \tag{21a}$$

$$\frac{\mu}{2aS\log(L/a)}|v_3|\lesssim\epsilon, \tag{21b}$$

$$\frac{\mu}{S}|\omega_3|\lesssim\epsilon, \tag{21c}$$

where $\mathbf{v}=v_k\hat{\mathbf{e}}_k$ and $\boldsymbol{\omega}$ is defined by $\frac{\partial\hat{\mathbf{e}}_k}{\partial t}=\boldsymbol{\omega}\times\hat{\mathbf{e}}_k$.

V. CONCLUSION

The primary results of this work indicate that the traditional approach to dealing with viscous drag forces by prescribing them as body forces and using zero surface stress to derive the torque-bend relations [Eq. (12)] is in good agreement with a precise treatment of these forces as surface tractions. However, handling viscous drag as a surface force leads naturally to bounds on the filament velocity [Eqs. (21a)–(21c)]. Specifically, we find that the velocity must be much less than aS/μ. As we mentioned in Sec. III, this condition can be recast in terms of the dimensionless ratio $\mathrm{Sp}^4/\epsilon^2<1$; however, this dimensionless form is not entirely accurate as the "sperm number" depends on the Young's modulus, not the shear modulus. Typical biofilaments have elastic moduli in the range from 1 MPa for bacterial cell walls [31] up to a few hundred MPa for DNA and bacterial flagella [50,51]. While these moduli represent the Young's moduli, typical materials have a Poisson ratio between 0 and 0.5, and, therefore, the shear modulus is only two to three times smaller than the Young's modulus [52]. If we consider biofilaments in water, $\mu=10^{-3}$ pN s/μm^2, then the velocity must be much less than 10^7–10^8 μm/s for most biofilaments. Since this velocity far exceeds the maximal velocities that can be achieved by most biofilaments, Kirchhoff rod theory can be accurately used to treat the dynamics of most filamentary biological structures.

There is, however, a potential consequence of the fact that the velocity bound depends on the shear modulus, as opposed to the Young's modulus. The bacterium *Spiroplasma* has received a fair degree of attention recently [53–56]. These bacteria are wall-less: They have a bilayer membrane that separates the cytoplasm from the external environment, but unlike most other bacteria they do not have a cell wall [57]. *Spiroplasma* swim by propagating chirality flips along the length of their cell body [54]. Because the cell body is *ds* defined by only a bilayer membrane, which is a liquid crystal, one expects there to be a finite bending modulus for the cell, but the shear modulus could be negligible or zero (however, there are cytoskeletal filaments that may impart an effective shear modulus to the cell body [58,59]). Therefore, for these cells, the bound on the velocity being proportional to the shear modulus may imply that the Kirchhoff rod equations will not provide an accurate fluid-structure model for the swimming of these bacteria. While our results here show that in most cases biofilaments can be accurately modeled using the traditional Kirchhoff rod equations with fluid resistance treated as a body force, for some realistic cases, a more detailed description may be required to capture the overdamped dynamics of the system.

ACKNOWLEDGMENTS

This work was partially supported by National Institutes of Health Grant No. NIH RO1 GM072004 (C. W.) and the NSF-AWM Mentoring Travel Grant (E. S.).

[1] M. D. Barkley and B. H. Zimm, J. Chem. Phys. **70**, 2991 (1979).
[2] C. J. Benham, Biopolymers **18**, 609 (1979).
[3] C. J. Benham, Proc. Natl. Acad. Sci. USA **76**, 3870 (1979).
[4] D. J. Dichmann, L. Y, and J. H. Maddocks, IMA Volume of Mathematics and its Applications **82**, 71 (1996).
[5] T. C. Bishop and Z. O. Oleksandr, J. Biomol. Struct. Dyn. **19**, 877 (2002).
[6] K. Hu, B. Math. Biol. **67**, 197 (2005).
[7] R. E. Goldstein and S. A. Langer, Phys. Rev. Lett. **75**, 1094 (1995).
[8] S. Lim, Phys. Fluids **22**, 4104 (2010).
[9] P. K. Purohit, J. Mech. Phys. Solids **56**, 1715 (2008).
[10] A. F. Fonseca and M. A. M. de Aguiar, Phys. Rev. E **63**, 016611 (2000).
[11] P. Nelson, Proc. Natl. Acad. Sci. USA **96**, 14342 (1999).
[12] S. Goyal, N. C. Perkins, and C. L. Lee, J. Comp. Phys. **209**, 371 (2005).
[13] S. Goyal, N. C. Perkins, and C. L. Lee, Int. J. Nonlinear Mech. **43**, 1121 (2008).
[14] I. Klapper, J. Comp. Phys. **125**, 325 (1996).
[15] Y. Yang, I. Tobias, and W. K. Olson, J. Chem. Phys. **98**, 1673 (1992).
[16] E. M. Strawbridge, Ph.D. thesis, University of California, Davis, 2009.
[17] C. J. Benham, A. G. Savitt, and W. R. Bauer, J. Mol. Biol. **316**, 563 (2002).
[18] C. J. Benham and S. P. Mielke, Annu. Rev. Biomed. Eng. **7**, 21 (2005).
[19] A. F. Fonseca, C. P. Malta, and M. A. M. de Aguiar, Physica A **352**, 547 (2005).
[20] A. F. Fonseca, C. P. Malta, and D. S. Galvao, J. Appl. Phys. **99**, 094310 (2006).
[21] R. E. Goldstein, A. Goriely, G. Huber, and C. W. Wolgemuth, Phys. Rev. Lett. **84**, 1631 (2000).
[22] S. A. Koehler and T. R. Powers, Phys. Rev. Lett. **85**, 4827 (2000).

[23] J. F. Marko and E. D. Siggia, Phys. Rev. E **52**, 2912 (1995).
[24] Y. Shi and J. E. Hearst, J. Chem. Phys. **101**, 5186 (1994).
[25] C. Fang-Yen *et al*., Proc. Natl. Acad. Sci. USA **107**, 20323 (2010).
[26] J. Korta *et al*., J. Exper. Biol. **210**, 2383 (2007).
[27] J. Sznitman *et al*., Exp. Mech. **50**, 1303 (2010).
[28] J. Sznitman *et al*., Biophys. J. **98**, 617 (2010).
[29] S. Lim, Y. Kim, and D. Swigon, Proc. R. Soc. A **467**, 569 (2011).
[30] J. Keller and S. I. Rubinow, Biophys. J. **16**, 151 (1976).
[31] W. Kan and C. W. Wolgemuth, Biophys. J. **93**, 54 (2007).
[32] C. W. Wolgemuth, T. R. Powers, and R. E. Goldstein, Phys. Rev. Lett. **84**, 1623 (2000).
[33] C. W. Wolgemuth, Biophys. J. **89**, 945 (2005).
[34] M. J. Shelley and T. Ueda, Physica D **146**, 221 (2000).
[35] N. H. Mendelson, J. E. Sarlls, C. W. Wolgemuth, and R. E. Goldstein, Phys. Rev. Lett. **84**, 1627 (2000).
[36] G. Kirchhoff, Journal für die reine und angewandte Mathematik **56**, 285 (1859).
[37] G. Kirchhoff, *Vorlesungen über mathematishe Physik, Mechanik*, Vorl. 28 (Teubner, Leipzig, 1876).
[38] A. Clebsch, *Theorie der Elasticität Fester Körper* (Teubner, Leipzig, 1862).
[39] A. Clebsch, *Théorie de l'Elasticité des Corps Solides* (Dunon, Paris, 1883).
[40] A. E. H. Love, *A Treatise on the Mathematical Theory of Elasticity* (Cambridge University Press, Cambridge, 1906).
[41] S. S. Antman, *Nonlinear Problems of Elasticity* (Springer, New York, 2005).
[42] E. H. Dill, Arch. Hist. Exact Sci. **44**, 1 (1992).
[43] E. Lauga and T. R. Powers, Rep. Prog. Phys. **72**, 096601 (2009).
[44] J. Gray and G. T. Hancock, J. Exp. Biol. **32**, 802 (1955).
[45] J. Lighthill, *Mathematical Biofluiddynamics* (SIAM, Philadelphia, 1975).
[46] R. E. Johnson and C. J. Brokaw, Biophys. J. **25**, 113 (1979).
[47] J. Keller and S. I. Rubinow, J. Fluid Mech. **75**, 705 (1976).
[48] R. Cortez and M. Nicholas, Com. Appl. Math. Comp. Sci. **7**, 33 (2012).
[49] T. R. Powers, Rev. Mod. Phys. **82**, 1607 (2010).
[50] H. Kojima, A. Ishijima, and T. Yanagida, Proc. Natl. Acad. Sci. USA **91**, 12962 (1994).
[51] C. Dombrowski *et al*., Biophys. J. **96**, 4409 (2009).
[52] L. Landau and E. Lifshitz, *Theory of Elasticity*, 3rd ed. (Butterworth-Heinemann, London, 1986).
[53] R. Gilad, A. Porat, and S. Trachtenberg, Mol. Microbiol. **47**, 657 (2003).
[54] J. W. Shaevitz, J. Y. Lee, and D. A. Fletcher, Cell **122**, 941 (2005).
[55] H. Wada and R. R. Netz, Phys. Rev. Lett. **99**, 108102 (2007).
[56] J. Yang, C. W. Wolgemuth, and G. Huber, Phys. Rev. Lett. **102**, 218102 (2009).
[57] S. Trachtenberg, J. Mol. Microbiol. Biotechnol. **7**, 78 (2004).
[58] S. Trachtenberg, R. Gilad, and N. Geffen, Mol. Microbiol. **47**, 671 (2003).
[59] J. Kurner, A. S. Frangakis, and W. Baumeister, Science **307**, 436 (2005).